Memory and Universality in Interface Growth

Jacopo De Nardis,[1,*] Pierre Le Doussal,[2,†] and Kazumasa A. Takeuchi[3,‡]
[1]Département de Physique, Ecole Normale Supérieure, PSL Research University, CNRS, 24 rue Lhomond, 75005 Paris, France
[2]CNRS-LPTENS, Ecole Normale Supérieure, PSL Research University, 24 rue Lhomond, 75005 Paris, France
[3]Department of Physics, Tokyo Institute of Technology, 2-12-1 Ookayama, Meguro-ku, Tokyo 152-8551, Japan
(Received 2 December 2016; published 21 March 2017)

Recently, very robust universal properties have been shown to arise in one-dimensional growth processes with local stochastic rules, leading to the Kardar-Parisi-Zhang (KPZ) universality class. Yet it has remained essentially unknown how fluctuations in these systems correlate at different times. Here, we derive quantitative predictions for the universal form of the two-time aging dynamics of growing interfaces and we show from first principles the breaking of ergodicity that the KPZ time evolution exhibits. We provide corroborating experimental observations on a turbulent liquid crystal system, as well as a numerical simulation of the Eden model, and we demonstrate the universality of our predictions. These results may give insight into memory effects in a broader class of far-from-equilibrium systems.

DOI: 10.1103/PhysRevLett.118.125701

Introduction.—Nonequilibrium dynamics is ubiquitous in nature, and takes diverse forms, such as avalanche motion in magnets and vortex lines [1,2], ultraslow relaxation in glasses [3,4], unitary evolution towards thermalization in isolated quantum systems [5], coarsening in phase ordering kinetics [6], and flocking in living matter [7]. Prominent examples are growth phenomena, which abound in physics [8–12], biology [8,13,14], and beyond [15]. As some of these systems try to reach local equilibrium or stationarity, a great variety of behaviors can occur, such as aging dynamics and memory of past evolution [1,4,6,16]. How universal and generic these behaviors are is a fundamental question [16].

One important example of growth arises when a stable phase of a generic system expands into a nonstable (or metastable) one, in the presence of noise. While spreading, the interface separating the two phases develops many nontrivial geometric and statistical features. A universal behavior then emerges, unifying many growth phenomena into a few universality classes, irrespective of their microscopic details. The most generic one, for local growth rules, is the celebrated Kardar-Parisi-Zhang (KPZ) class, now substantiated by many experimental examples, such as growing turbulence of a liquid crystal [9–11], propagating chemical fronts [15], paper combustion [12], and bacteria colony growth [13]. For one-dimensional interfaces growing in a plane, as studied in many experiments, it is characterized by the following KPZ equation [17]:

$$\partial_t h(x,t) = \nu \partial_x^2 h(x,t) + \frac{\lambda_0}{2}[\partial_x h(x,t)]^2 + \sqrt{D}\eta(x,t), \quad (1)$$

which describes the motion of an interface of height $h(x,t)$ at point $x \in \mathbb{R}$ at time t, driven by a unit space-time white noise $\eta(x,t)$. Recently, this problem became an outstanding example where a wealth of universal statistical properties can be solved exactly, from the KPZ equation and related lattice models [18–28]. At large time, the height evolves as $h(0,t) \simeq v_\infty t + (\Gamma t)^{1/3}\tilde{h}_t$ with system-dependent parameters v_∞, Γ, and a stochastic variable $\tilde{h}_t$ that carries universal information of the fluctuations. Remarkably, in the limit $t \to \infty$, $\tilde{h}_t$ follows one of a few non-Gaussian universal distributions, selected only by the global geometric shape of the initial condition $h(x, t=0)$: in particular, the GUE Tracy-Widom distribution [29] $F_2(\sigma)$, when $h(x,0)$ is narrowly curved [droplet initial condition [20–23], see Fig. 1(a)] and its GOE variant $F_1(\sigma)$, when $h(x,0)$ is a flat surface [24]. These two distributions also describe the fluctuations of the largest eigenvalue of a Gaussian random matrix drawn from the unitary (GUE) or orthogonal (GOE) ensembles, revealing a striking connection to the theory of random matrices [19,30]. An additional universal distribution, the Baik-Rains distribution [18], characterizes the stationary state of the growth and can be reached [25] by choosing $h(x,0)$ as Brownian motion in x. This geometry-dependent universality was tested and confirmed experimentally, in studies on growing interfaces of liquid-crystal turbulence [9–11]. The experiments also allowed us to investigate time-correlation properties that were inaccessible by analytical approaches. This revealed an anomalous memory effect for the droplet case [11], by which fluctuations in h keep indefinite memory of the past, in contrast to the naive expectation that memory is eventually lost. This persistence of memory, signaling ergodicity breaking in the time evolution of the droplet case, is quantified by the long time limit of the covariance that remains strictly positive [11,31] $\lim_{\Delta\to\infty}\lim_{t_1\to\infty} C(t_1, t_1(1+\Delta)) > 0$, where $C(t_1,t_2) = \mathrm{cov}[h(0,t_1), h(0,t_2)]$. Theoretically, however, such two-time quantities remained so far analytically intractable, except for a few exceptional results [32,33] that however are too involved to produce practical predictions. Since experiments and simulations are always

confronted with relatively limited ranges of time t_1 and the ratio Δ, while the suspected ergodicity breaking can only be addressed in the limits $t_1 \to \infty$ then $\Delta \to \infty$, a theory that can directly deal with these asymptotic limits, and also make a bridge to finite-time observations through predictions, is a crucial missing facet of the problem. Here, we provide the first theoretical results for the correlations at two different times in the infinite time limit of the KPZ equation, and we analytically prove the persistence of correlations that was previously observed in finite-time experiments [11]. This shows that a fraction of the fluctuations of the droplet KPZ interface, mostly the ones with large and positive rescaled height, maintain their configurations stable during the time evolution, as also is made clear below from a dual directed polymer picture. This translates into an ergodicity breaking in all the growth processes with the droplet initial condition.

Two-time JPDF.—We address the problem by deriving an analytical result for the joint probability density function (JPDF) of the height h at two different times t_1 and $t_2 = (1+\Delta)t_1$, with the droplet initial condition, see Fig. 1. It is valid in a wide range of parameters and agrees remarkably well with experimental and numerical data (see below). We focus on the limit $t_1, t_2 \to \infty$ with their ratio $t_2/t_2 = 1+\Delta$ kept finite, so that the obtained correlations are expected to be universal within the KPZ class. More precisely, we compute the JPDF for the rescaled height

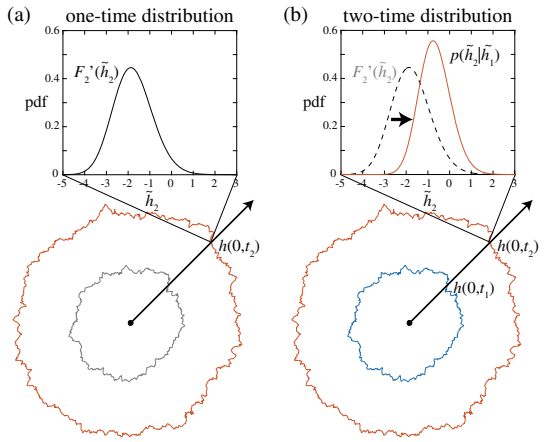

FIG. 1. Sketch of the KPZ time evolution: the two rough lines show the expanding KPZ height, describing the edge of a growing circular region. Note that, for isotropic systems, the local radius corresponds to $h(0,t)$ in any angular direction. (a) The fluctuations of the interface at time t_2 are described by the GUE Tracy-Widom distribution $F_2'(\tilde{h}_2)$ with the rescaled height $\tilde{h}_2 = \tilde{h}_{t_2} = (h(0,t_2) - v_\infty t_2)/(\Gamma t_2)^{1/3}$. (b) Given the fluctuations of the height at a previous time $t_1 = t_2(1+\Delta)^{-1}$ along the same angular direction (black arrow), the two-time conditional probability density $p(\tilde{h}_2|\tilde{h}_1)$ (red line) measures the probability of observing a fluctuation value $\tilde{h}_2$ at time t_2, given the value of $\tilde{h}_1$ at the previous time t_1 (the inset shows the conditional distribution for $\tilde{h}_1 = 0$).

$\tilde{h}_1 = \tilde{h}_{t_1} = (h(0,t_1) - v_\infty t_1)/(\Gamma t_1)^{1/3}$ and the rescaled two-time height difference $\tilde{h}_{12} = (h(0,t_2) - h(0,t_1) - v_\infty t_1 \Delta)/(\Gamma t_1 \Delta)^{1/3}$. It is defined as

$$P_\Delta(\sigma_1,\sigma)d\sigma_1 d\sigma = \lim_{t_1\to\infty}\{\mathrm{Prob}(\sigma_1 \le \tilde{h}_1 \le \sigma_1 + d\sigma_1, \sigma \le \tilde{h}_{12} \le \sigma + d\sigma)\} \quad (2)$$

and quantifies how much memory of the configuration at the earlier time t_1 is retained at the later time t_2, as illustrated in Fig. 1(b). It allows us to calculate the conditional cumulants $\langle \tilde{h}_{12}^n \rangle^{\mathrm{c}}_{\tilde{h}_1 > \sigma_{1c}}$, i.e., the cumulants of the variable $\tilde{h}_{12}$ conditioned to realizations with $\tilde{h}_1$ larger than some fixed value σ_{1c}. It also allows us to predict the rescaled covariance under the same conditioning, defined as

$$C_{\Delta,\sigma_{1c}} = \frac{C(t_1,t_2)_{\tilde{h}_1>\sigma_{1c}}}{C(t_1,t_1)_{\tilde{h}_1>\sigma_{1c}}} = 1 + \Delta^{1/3}\frac{\mathrm{cov}[\tilde{h}_1,\tilde{h}_{12}]_{\tilde{h}_1>\sigma_{1c}}}{\langle \tilde{h}_1^2 \rangle^{\mathrm{c}}_{\tilde{h}_1>\sigma_{1c}}}. \quad (3)$$

These quantities, computed here analytically for the first time, allow us to probe memory effects and quantify the breaking of ergodicity in the dynamics. In particular, Eq. (3) quantifies how much memory of the fluctuations with rescaled amplitudes larger than σ_{1c} is kept at later times and it recovers the full two-time covariance $C(t_1,t_2)$ in the limit $\sigma_{1c} = -\infty$.

Solution via the directed polymer.—To derive a numerically tractable expression for the JPDF (2), we exploit the fact [34] that the KPZ equation is equivalent to a (statistical mechanics) problem of space-time paths (i.e., "growth histories") in a random potential, which is further mapped into a quantum problem of bosons (see Fig. 2). From now on we use the scales $x^* = (2\nu)^3/D\lambda_0^2$, $t^* = (2(2\nu)^5)/(D^2\lambda_0^4)$, $h^* = (2\nu)/\lambda_0$ as units of space, time, and height, respectively. In other words, x/x^*, t/t^*, h/h^* are simply denoted by x, t, h, respectively (this amounts to setting $\nu = 1, \lambda_0 = 2$, and $D = 2$ in the KPZ equation, which leads to $\Gamma = 1$). In these units, from Eq. (1), the function $Z(x,t) = e^{h(x,t)}$ satisfies a linear stochastic equation; thus, it can be written as a sum over space-time paths and can be interpreted as the canonical partition sum of a directed polymer (DP) with endpoints $(0,0)$ and (x,t) in a unit white noise random potential $-\sqrt{2}\eta$ [see Fig. 2(a)]

$$Z(x,t|y,0) = \int_{x(0)=0}^{x(t)=x} Dx e^{-\int_0^t d\tau[\frac{1}{4}(dx/d\tau)^2 - \sqrt{2}\eta(x(\tau),\tau)]}.$$

The function $P_\Delta(\sigma_1,\sigma)$ maps to the JPDF of the free energies of two DPs starting both in (0, 0) but ending in $(0,t_1)$ and $(0, t_2 = t_1(1+\Delta))$: in Fig. 2(a) is shown a typical configuration of these two paths, which tend to visit the lower valleys of the potential (bluer regions), i.e., faster growth regions, compatible with their boundary conditions and kinetic energies, which tend to minimize their length. The JPDF (2) is obtained [35] from the joint integer moments $\langle Z(0,t_1)^{n_1} Z(0,t_2)^{n_2} \rangle$, averaged over realizations

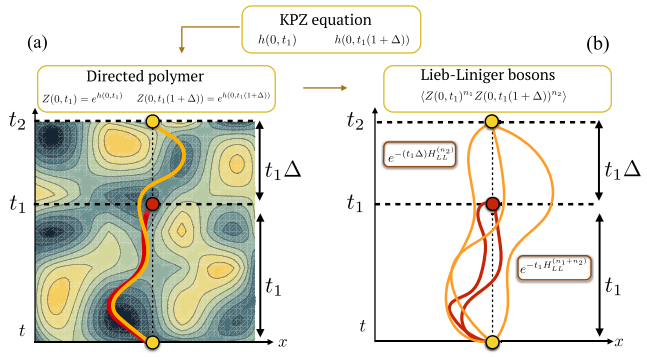

FIG. 2. (a) Representation of the mapping from the height $h(x,t)$ in the KPZ equation (1) to the free energy of a directed polymer in a random potential. Shown here is a typical configuration of two polymers, which tend to visit the lower valleys of the potential (bluer regions). The two paths tend to overlap in the time interval $[0,t_1]$, accounting for ergodicity breaking (see text). (b) Mapping (via the replica method) to a quantum mechanical transition amplitude of attractive one-dimensional bosons.

of η. They are given by the quantum mechanical amplitude of the following process [see Fig. 2(b)]: n_1+n_2 bosons with a pairwise attractive potential evolve from $x=0$ in imaginary time up to time t_1. At $t=t_1$, n_1 of them are annihilated at $x=0$, while the other n_2 keep evolving up to $t=t_1(1+\Delta)$, at which they are all finally destroyed at $x=0$ [Eq. (S3) in Ref. [35]]. Their Hamiltonian is the Lieb-Liniger Hamiltonian with attractive interaction

$$H_{\mathrm{LL}}^{(n)}=-\sum_{j=1}^{n}\partial_{x_j}^2-2\sum_{i<j}^{n}\delta(x_i-x_j)-\frac{n}{12}, \tag{4}$$

extensively studied recently in the context of integrable out-of-equilibrium dynamics [38–40]. Integrability of this dual quantum model allows us to derive an analytical expression for $P_\Delta(\sigma_1,\sigma)$, in the form $P_\Delta(\sigma_1,\sigma)=P_\Delta^{(1)}(\sigma_1,\sigma)[1+\mathcal{O}(e^{-(4/3)\sigma_1^{3/2}})]$ with $P_\Delta^{(1)}(\sigma_1,\sigma)$ exactly determined in this work [35]. It is written as a trace of kernels acting on $\mathbb{R}\times\mathbb{R}$:

$$P_\Delta^{(1)}(\sigma_1,\sigma)=(\partial_{\sigma_1}\partial_\sigma-\Delta^{-1/3}\partial_\sigma^2)\times\{F_2(\sigma)\mathrm{Tr}[\Delta^{1/3}\Pi_\sigma K_{\sigma_1}^{\Delta}\Pi_\sigma(I-\Pi_\sigma K_{\mathrm{Ai}}\Pi_\sigma)^{-1}-\Pi_{\sigma_1}K_{\mathrm{Ai}}]\}, \tag{5}$$

where Π_σ projects on the interval $[\sigma,+\infty]\in\mathbb{R}$, I is the identity operator, and ∂_σ denotes partial derivatives. The expression involves the well-known Airy kernel $K_{\mathrm{Ai}}(r,r')=\int_0^\infty dz\mathrm{Ai}(r+z)\mathrm{Ai}(r'+z)$ from random matrix theory [29] and a novel kernel

$$K_{\sigma_1}^{\Delta}(r,r')=\int_0^\infty dz_1dz_2\mathrm{Ai}(-z_1+r)\mathrm{Ai}(-z_2+r')\times K_{\mathrm{Ai}}(z_1\Delta^{1/3}+\sigma_1,z_2\Delta^{1/3}+\sigma_1). \tag{6}$$

The formula (5) can be easily evaluated numerically for any value of σ_1 inside its expected validity range (specifically $\sigma_1\gtrsim-1.5$). This allows us to perform direct tests of the theoretical predictions, both experimentally and numerically, without any fitting parameters. Experimentally, we study growing interfaces of electrically driven liquid-crystal

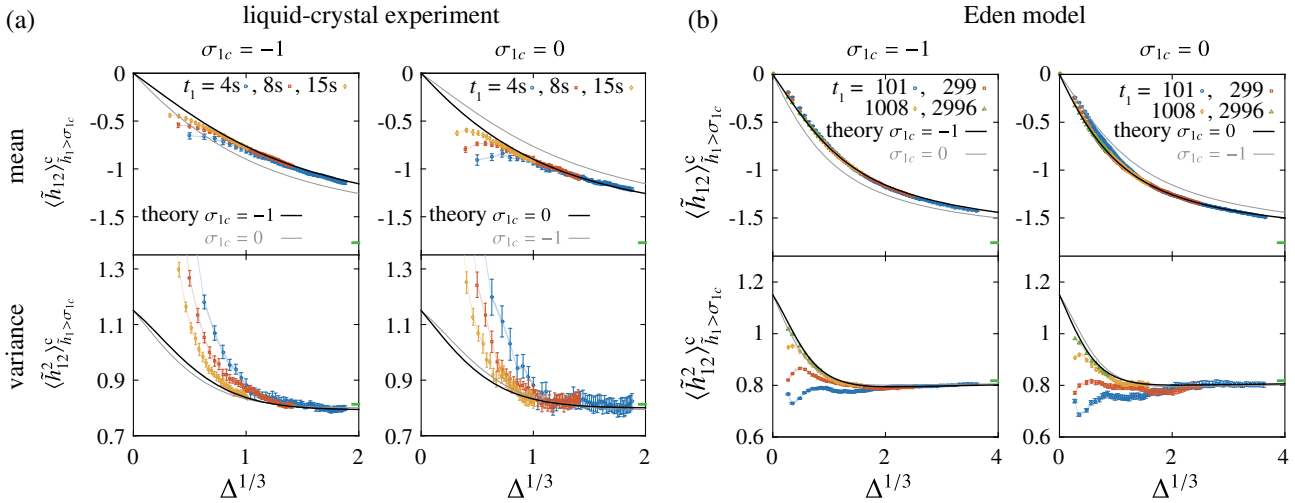

FIG. 3. Test of the theoretical prediction for the conditional mean $\langle\tilde{h}_{12}\rangle^{\mathrm{c}}_{\tilde{h}_1>\sigma_{1c}}$ and variance $\langle\tilde{h}_{12}^2\rangle^{\mathrm{c}}_{\tilde{h}_1>\sigma_{1c}}$ with the liquid-crystal experiment (a) and the Eden-model simulation (b). Here, the results for $\sigma_{1c}=-1$ and 0 are shown (see also Fig. S3 in Ref. [35] for $\sigma_{1c}=-1.5$). Data at different t_1 are shown in different colors and symbols. The regions of overlapped data indicate the asymptotic Δ dependence, which is found to be in excellent agreement with the theoretical predictions (black lines), without any fitting parameter. For comparison, the theoretical curves with another value of σ_{1c} are shown by gray thin lines. The error bars indicate the standard errors, and the shaded areas show the uncertainty due to the estimation error in v_∞ and Γ. To reduce the effect of finite-time corrections, here we used such realizations that satisfy $\tilde{h}_1>\tilde{h}_{1c}$ with $\mathrm{Prob}[\tilde{h}_1\geq\tilde{h}_{1c}]=1-F_2(\sigma_{1c})$. The deviation of the nonoverlapped data is due to finite-time corrections, which decay as t_1^{-1}, see Fig. S4 in Ref. [35]. Note that the asymptotic theoretical curves converge to the Baik-Rains values (mean 0, variance 1.1504) at $\Delta\to0$ and the GUE Tracy-Widom values (mean -1.7711, variance 0.8132, indicated in the figures by the green bars) at $\Delta\to\infty$.

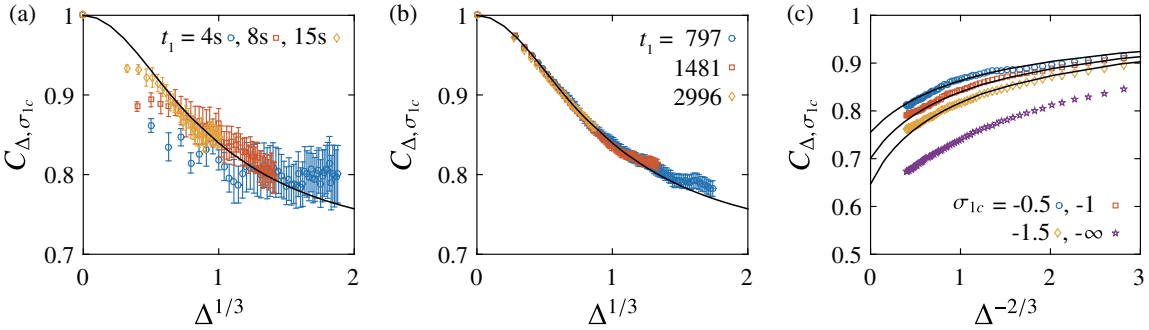

FIG. 4. The conditional covariance $C_{\Delta,\sigma_{1c}} = C(t_1,t_2)_{\tilde{h}_1>\sigma_{1c}}/C(t_1,t_1)_{\tilde{h}_1>\sigma_{1c}}$ [Eq. (3)]. (a),(b) Experimental (a) and numerical (b) results for $\sigma_{1c} = -1$ and with varying t_1 (symbols), compared with the theoretical prediction (black line). The error bars indicate the standard errors. To reduce the effect of finite-time corrections, here we used such realizations that satisfy $\tilde{h}_1 > \tilde{h}_{1c}$ with $\text{Prob}[\tilde{h}_1 \geq \tilde{h}_{1c}] = 1 - F_2(\sigma_{1c})$. (c) Numerical data for $t_1 = 1008$ and for $\sigma_{1c} = -0.5$, -1, -1.5, and $-\infty$ (unconditioned). Error bars are omitted here for the sake of visibility. The black lines indicate the theoretical predictions for finite σ_{1c}. At large Δ and for any σ_{1c} they converge to their asymptotic values as $C_{\Delta\to\infty,\sigma_{1c}} + A_{\sigma_{1c}}\Delta^{-2/3} + B_{\sigma_{1c}}\Delta^{-1} + \cdots$. For $\sigma_{1c} = -\infty$ (the unconditioned case), the theory suggests a strictly positive asymptotic value, specifically $C_{\infty,-\infty} \approx 0.6$, which is consistent with the trend of the unconditioned data set in panel (c) (purple stars).

turbulence, which were previously shown to be in the KPZ class [9–11] (see Refs. [11,35] for details). We use 955 interfaces, generated from a turbulent nucleus (droplet initial condition) triggered by a laser, for which the nonuniversal parameters v_∞ and Γ were determined with high precision [11] and used to obtain the rescaled variables. Then we measure the conditional cumulants $\langle \tilde{h}_{12}^n \rangle^c_{\tilde{h}_1>\sigma_{1c}}$ with different t_1 [Fig. 3(a)]. Their asymptotic forms, which are indicated by the overlapping of data sets, are found to show an excellent agreement with the theoretical predictions [Fig. 3(a) and Fig. S3(a) in Ref. [35]]. For a further test, we carry out numerical simulations of the off-lattice Eden model [41] (5000 realizations; see Ref. [35] for details) and the same quality of agreement is obtained [Fig. 3(b) and Fig. S3(b) in Ref. [35]]. We also measure the conditional covariance (3) and find agreement both experimentally and numerically (Fig. 4). This indicates that our predictions describe the universal time correlation of the droplet KPZ interfaces. Moreover, our theory shows analytically for the first time the crossover between different probability distributions for $\tilde{h}_{12}$, as Δ varies (see Fig. 5). In the limit of close times, $t_2/t_1 \to 1^+$, the JPDF (5) factorizes and $\tilde{h}_1$, $\tilde{h}_{12}$ become two independent random variables following, respectively, the GUE Tracy-Widom and Baik-Rains distributions. The emergence of the Baik-Rains distribution is direct evidence of the approach to the KPZ stationary state when $t_2/t_1 \to 1^+$ [31]. As time separation increases, a nontrivial aging form develops and for $\Delta \to \infty$ the joint statistics factorizes into the product of two GUE Tracy-Widom distributions. The next order correction, of order $\mathcal{O}(\Delta^{-1/3})$, gives access to the asymptotic value of the persistent correlation $C_{\Delta\to\infty,\sigma_{1c}}$: as σ_{1c} decreases from $+\infty$ to $-\infty$, i.e., the unconditioned case, it is predicted to decrease from 1 to a strictly positive value estimated to be ≈ 0.6 [35], which is consistent with our numerical data [Fig. 4(c), purple stars].

The directed polymer or growth-history path representation enlightens this ergodicity breaking phenomenon. As illustrated in Fig. 2, the two polymers tend to visit the same minima of the random potential thus sharing a finite fraction, i.e., the overlap $0 < q < 1$, of their paths (growth histories) in the time interval $[0, t_1]$. Indeed, in the large time limit it is known that the DP partition sum from (0,0) to (x, t) is dominated by the path between these two points, which minimize the DP energy. Since two optimal paths in the same potential necessarily coincide once they meet, and since both polymers must pass through (0, 0), a finite mean overlap q is expected. This effect thus combines an energetic and a geometric origin and translates into a finite two-time correlation even in the limit $t_2 \gg t_1$. Our theory further quantifies the energetic or height level aspect: as σ_{1c} is increased, noise realizations with large and positive height fluctuations are selected in the interval $0 \leq t \leq t_1$. These correspond to realizations of the random potential deeper than average; therefore, the shared fraction q of the path of the two polymers approaches unity, and the memory becomes perfect $C_{\Delta\to\infty,\sigma_{1c}} \to 1$. This is consistent with the experimental and

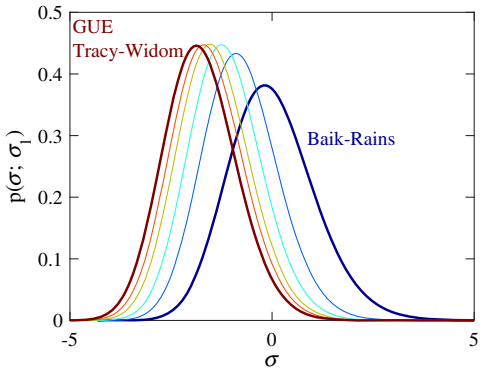

FIG. 5. Predicted crossover from the Baik-Rains distribution ($\Delta \to 0$, i.e., $t_2/t_1 \to 1^+$) to the GUE Tracy-Widom distribution ($\Delta \to \infty$, i.e., $t_2/t_1 \to \infty$), for the conditional probability of the rescaled height difference $\tilde{h}_{12}$. Plotted here is the normalized conditional probability $P^{(1)}_\Delta(\sigma_1 = 0, \sigma)/F_2'(\sigma_1 = 0)$ with $\Delta^{1/3} = 0, 0.7, 1.4, 2.8, 5.6, \infty$ from right to left.

numerical observation (Fig. 4). Note that, interestingly enough, also the negative height fluctuations can lead to a finite mean overlap q, since the DP tends to minimize locally its energy even in a higher than average potential.

Conclusions.—In summary, our results represent the first analytical theoretical predictions on the universal aging form for the two-time correlations of the KPZ equation (1) that remarkably fit experimental and numerical data. It therefore gives a quantitative prediction for the crossover of the distribution of the fluctuations $\tilde{h}_{12}$ to the stationary state (i.e., the Baik-Rains distribution) as $t_2/t_1 \to 1^+$, and confirms for the first time the breaking of ergodicity in the KPZ time evolution from the droplet initial condition. Both are expected to be universal properties shared by all growth processes in the KPZ class. This universality in multitime correlations, accompanied with ergodicity breaking, could be explored in a broader class of growth problems both within and beyond the KPZ class [42]. In expanding geometries we expect similar persistence of memory when the spatial scale of dynamical correlations, $x \sim t_1^{\zeta}$ ($\zeta = 2/3$ for KPZ), grows slower than the expanding substrate radius (here $\sim t_1$). It should also be relevant for other nonequilibrium systems, such as driven Bose-Einstein condensates [43] and genetic segregation in expanding bacterial colonies [14], both shown to relate to KPZ.

We thank P. Calabrese, I. Corwin, and K. Johansson for discussions. This work is supported in part by KAKENHI from Japan Society for the Promotion of Science, No. JP25103004, No. 16H04033, and No. 16K13846 (K. A. T.), Laboratory of Excellence ENS-ICFP:ANR-10-LABX-0010/ANR-10-IDEX-0001-02 PSL* (J. D. N.), and the National Science Foundation under Grant No. NSF PHY11-25915.

*jacopo.de.nardis@phys.ens.fr
†ledou@lpt.ens.fr
‡kat@kaztake.org

[1] D. Xu, L. Guohong, E. Y. Andrei, M. Greenblatt, and P. Shuk, Nat. Phys. **3**, 111 (2007).
[2] S. Papanikolaou, F. Bohn, R. L. Sommer, G. Durin, S. Zapperi, and J. P. Sethna, Nat. Phys. **7**, 316 (2011).
[3] J. Kurchan, Nature (London) **433**, 222 (2005).
[4] L. F. Cugliandolo, *Proceedings of the Les Houches Summer School, Session number LXXVII*, edited by J.-L. Barrat, M. Feigelman, J. Kurchan, and J. Dalibard (Springer-Verlag, Heidelberg, 2003).
[5] J. Eisert, M. Friesdorf, and C. Gogolin, Nat. Phys. **11**, 124 (2015).
[6] A. J. Bray, S. N. Majumdar, and G. Schehr, Adv. Phys. **62**, 225 (2013).
[7] L. Chen, C. F. Lee, and J. Toner, Nat. Commun. **7**, 12215 (2016).
[8] A. L. Barabasi and H. E. Stanley, *Fractal Concepts in Surface Growth* (Cambridge University Press, Cambridge, England, 1995).
[9] K. A. Takeuchi and M. Sano, Phys. Rev. Lett. **104**, 230601 (2010).
[10] K. A. Takeuchi, M. Sano, T. Sasamoto, and H. Spohn, Sci. Rep. **1**, 34 (2011).
[11] K. A. Takeuchi and M. Sano, J. Stat. Phys. **147**, 853 (2012).
[12] J. Maunuksela, M. Myllys, O.-P. Kähkönen, J. Timonen, N. Provatas, M. J. Alava, and T. Ala-Nissila, Phys. Rev. Lett. **79**, 1515 (1997).
[13] J. Wakita, H. Itoh, T. Matsuyama, and M. Matsushita, J. Phys. Soc. Jpn. **66**, 67 (1997).
[14] O. Hallatschek, P. Hersen, S. Ramanathan, and D. R. Nelson, Proc. Natl. Acad. Sci. U.S.A. **104**, 19926 (2007).
[15] S. Atis, A. K. Dubey, D. Salin, L. Talon, P. Le Doussal, and K. J. Wiese, Phys. Rev. Lett. **114**, 234502 (2015).
[16] M. Henkel, J. D. Noh, and M. Pleimling, Phys. Rev. E **85**, 030102(R) (2012).
[17] M. Kardar, G. Parisi, and Y. C. Zhang, Phys. Rev. Lett. **56**, 889 (1986).
[18] J. Baik and E. M. Rains, J. Stat. Phys. **100**, 523 (2000).
[19] M. Prahofer and H. Spohn, Phys. Rev. Lett. **84**, 4882 (2000).
[20] T. Sasamoto and H. Spohn, Phys. Rev. Lett. **104**, 230602 (2010).
[21] P. Calabrese, P. Le Doussal, and A. Rosso, Europhys. Lett. **90**, 20002 (2010).
[22] V. Dotsenko, Europhys. Lett. **90**, 20003 (2010).
[23] G. Amir, I. Corwin, and J. Quastel, Commun. Pure Appl. Math. **64**, 466 (2011).
[24] P. Calabrese and P. Le Doussal, Phys. Rev. Lett. **106**, 250603 (2011).
[25] T. Imamura and T. Sasamoto, Phys. Rev. Lett. **108**, 190603 (2012).
[26] P. Le Doussal, S. N. Majumdar, A. Rosso, and G. Schehr, Phys. Rev. Lett. **117**, 070403 (2016).
[27] P. Le Doussal, S. N. Majumdar, and G. Schehr, Europhys. Lett. **113**, 60004 (2016).
[28] A. De Luca and P. Le Doussal, Phys. Rev. E **93**, 032118 (2016).
[29] C. A. Tracy and H. Widom, Commun. Math. Phys. **159**, 151 (1994).
[30] T. Kriecherbauer and J. Krug, J. Phys. A **43**, 403001 (2010).
[31] P. L. Ferrari and H. Spohn, SIGMA **12**, 074 (2016).
[32] V. Dotsenko, J. Stat. Mech. (2013) P06017.
[33] K. Johansson, Commun. Math. Phys. **351**, 441 (2017).
[34] M. Kardar, Nucl. Phys. **B290**, 582 (1987).
[35] See Supplemental Material at http://link.aps.org/supplemental/10.1103/PhysRevLett.118.125701 for further information on the theoretical results, descriptions of the experimental and numerical system, and Fig. S1–S4, which includes Refs. [36,37].
[36] F. Bornemann, Math. Comput. **79**, 871 (2010).
[37] S. G. Alves, T. J. Oliveira, and S. C. Ferreira, J. Stat. Mech. (2013) P05007.
[38] P. Calabrese and J.-S. Caux, Phys. Rev. Lett. **98**, 150403 (2007).
[39] M. Panfil, J. De Nardis, and J.-S. Caux, Phys. Rev. Lett. **110**, 125302 (2013).
[40] L. Piroli, P. Calabrese, and F. H. L. Essler, Phys. Rev. Lett. **116**, 070408 (2016).
[41] K. A. Takeuchi, J. Stat. Mech. (2012) P05007.
[42] I. S. S. Carrasco and T. J. Oliveira, Phys. Rev. E **94**, 050801 (2016).
[43] L. He, L. M. Sieberer, E. Altman, and S. Diehl, Phys. Rev. B **92**, 155307 (2015).